Journal of Photochemistry and Photobiology A: Chemistry 202 (2009) 214–220

Contents lists available at ScienceDirect

Journal of Photochemistry and Photobiology A: Chemistry

journal homepage: www.elsevier.com/locate/jphotochem

Mechanisms involved in the platinization of sol–gel-derived TiO_2 thin films

D. Riassetto[a], C. Holtzinger[a], M. Messaoud[a], S. Briche[a], G. Berthomé[b], F. Roussel[c], L. Rapenne[a], M. Langlet[a,*]

[a] LMGP (Grenoble Institute of Technology), Minatec, 3 Parvis Louis Neel, BP 257, 38016 Grenoble Cedex 1, France
[b] SIMAP (Grenoble Institute of Technology), BP 75, Domaine Universitaire, 38402 Saint Martin d'Hères, France
[c] CMTC (Grenoble Institute of Technology), BP 75, Domaine Universitaire, 38402 Saint Martin d'Hères, France

ARTICLE INFO

Article history:
Received 4 September 2008
Received in revised form
21 November 2008
Accepted 29 November 2008
Available online 11 December 2008

Keywords:
Photocatalysis
Photolysis
TiO_2
Sol–gel
Thin film
Platinum

ABSTRACT

Sol–gel TiO_2 thin films have been loaded with platinum nano-particles via their immersion within a Pt^{4+} precursor liquid solution exposed to UV light. Mechanisms involved in the photo-induced formation of platinum particles have been studied by UV/visible spectroscopy, X-ray photoelectron spectroscopy, energy dispersive X-ray analysis, scanning electron microscopy, and transmission electron microscopy. According to studied mechanisms, it is shown that the amount, size, and structural state of photo-generated platinum particles dispersed at a solid surface can flexibly be monitored.

1. Introduction

Platinum clusters loaded at the surface of TiO_2 photocatalysts strongly enhance the photocatalytic activity of titania through the formation of a Schottky barrier at the TiO_2/Pt interface, which promotes an efficient separation of holes and electrons charge carriers photo-generated under UV light. Though this effect has extensively been studied over the three past decades for powder TiO_2 photocatalysts, only very recent works report on the platinization of TiO_2 photocatalytic thin films [1–5]. Among various platinization methods used to functionalize powder TiO_2 photocatalysts, photo-metallization is one of the most employed [6–12]. This method is usually considered to rely on the reduction of a Pt^{4+} precursor, adsorbed at the TiO_2 surface, induced by electrons photo-generated in the TiO_2 conduction band under UV light, i.e. a photocatalytic reduction mechanism. In a recent work, we have shown that this method can be applied to platinize TiO_2 sol–gel films [13]. Photo-platinization was achieved using a chloro-platinic acid (CPA) precursor diluted in aqueous solution, which was then exposed to UV light in the presence of a TiO_2 sol–gel film. We showed that, in optimal conditions, photocatalytic activity of the platinized films (deduced using Orange G as a model molecule to be photocatalytically decomposed) could be increased by a factor 3 to 4 compared to a non-platinized film. These optimal conditions particularly rely on i/a water/ethanol mixture of 80/20 molar composition, which is used as a dilution medium of CPA during UV exposure, and ii/a heat-treatment performed after TiO_2 film platinization in a 110–400 °C thermal range. These conditions control the amount of loaded platinum and the metallization degree of platinum clusters, and allow preventing adsorption of other photo-decomposition by-products at the TiO_2 surface. Indeed, such adsorbed by-products can seriously alter the photocatalytic activity of TiO_2 films, in particular carbon monoxide, which arises from ethanol photo-decomposition and adsorbs at the platinum clusters, thus considerably reducing the platinum efficiency [13]. Despite promising results, these first studies still raise many questions, i.e. what are exact mechanisms involved in the photo-platinization of TiO_2 films, how these mechanisms influence different features such as platinum amount, size, and reduction degree, and how these latter features influence in turn the photocatalytic activity of TiO_2 films. In this article, we present more recent studies that provide new insights into these different aspects.

2. Experimental

2.1. TiO_2 sol and film preparations

Sol–gel TiO_2 films were deposited from a polymeric sol, which was prepared by mixing tetraisopropyl orthotitanate (TIPT;

* Corresponding author.
E-mail address: michel.langlet@inpg.fr (M. Langlet).

1010-6030/$ – see front matter © 2008 Elsevier B.V. All rights reserved.
doi:10.1016/j.jphotochem.2008.11.023

$Ti(C_3H_7O)_4$ from Fluka) with deionized water, hydrochloric acid, and absolute ethanol as a solvent. TIPT concentration in the solution was fixed at 0.4 M, and the TIPT/H_2O/HCl molar composition was 1/0.82/0.13. The sol was aged at room temperature for 2 days before first depositions, after what it could be used for several weeks in reproducible deposition conditions. Films were deposited at room temperature on (1 0 0) silicon wafers (3.3 cm × 3.3 cm) by spin-coating using a Suss Microtec RC8 apparatus. Prior to deposition, the substrates were cleaned with ethanol, then rinsed with deionised water, and dried with air spray. For each deposition, 300 μl of sol were spread on the substrate rotated at 3000 rpm. After liquid film deposition, the solvent rapidly evaporated and a solid film formed at ambient atmosphere through the well-known sol–gel polymerization route. A multi-layer procedure was adopted to fix the final oxide film thickness at around 250 nm. Each as-deposited single-layer film was heat treated in air for 2 min at 500 °C before deposition of a subsequent single-layer. The final 7-layer film was then heat treated at 500 °C for 2 h. Our previous works showed that such conditions yielded well-crystallized anatase TiO_2 films with good photocatalytic activity [14,15].

2.2. Photo-platinization conditions

Photo-platinization experiments were performed using CPA hexahydrate ($H_2PtCl_6{\cdot}6H_2O$ from Strem Chemicals) as a platinum precursor. CPA was first diluted in absolute ethanol to give a solution of 1.9 mM platinum concentration. The resulting solution was very stable and could be used for one year or more in reproducible conditions. Before platinization, this solution was further diluted in deionized water and absolute ethanol, with water/ethanol molar ratio of 80/20, and the final CPA content was varied from 23 to 860 μM. A volume of 100 ml of this solution was poured into a glass vessel opened to air. A titania-coated substrate was settled on a sample holder and immersed in this solution, the coated surface being oriented toward bottom of the glass vessel, at a distance of 8 mm. The solution was first stored in dark conditions for 1 h to reach equilibrated adsorption of CPA at the film surface. Sample and solution were then exposed to UV radiation arising from three UVA lamps (PLS 11W from Philips), essentially emitting at a 365 nm wavelength (negligible UVB/UVC emission) and located at 2 cm below the glass vessel bottom. UV exposure experiments were performed, for various durations ranging up to 15 h, in a climatic cabinet regulated at a 20 °C temperature and 40% relative humidity. Constant agitation of the solution was insured over UV exposure using a magnetic stirrer rotated at 500 rpm. After photo-platinization, films were rinsed with deionized water and subsequently heat treated in air at 110 °C for 2 h. Variations of this protocol have also been studied, which will be discussed in the text.

2.3. Characterization methods

Mechanisms occurring in the solutions exposed to UV light were analyzed by UV/visible spectroscopy, in a 200–1100 nm spectral range, using a Jasco V-530 spectrophotometer. Over UV exposure, small solution aliquots were periodically withdrawn for spectral measurement. Physico-chemical, morphological, and structural characterizations were performed using various techniques. A Philips XL 30 scanning electron microscope (SEM) operated at 6 kV was employed for energy dispersive X-ray (EDX) analyses. Surface imaging of platinized films was performed using a ZEISS Ultra 55 Field Emission Gun (FEG)-SEM operated at 20 kV. High-resolution transmission electron microscopy (TEM) observations were performed using a JEOL-2010 LaB_6 instrument operated at 200 keV. Surface chemical analysis was performed by X-ray photoelectron spectroscopy (XPS) using a XR3E2 apparatus from Vacuum Generator employing an Mg Kα source (1253.6 eV). Before collecting data, the samples were put in equilibrium for 24 h in an ultra high vacuum chamber (10^{-10} mbar). Photoelectrons were collected by a hemispherical analyzer at 30° and 90° take-off angles. The spectra were calibrated with the C1s peak at 284.7 eV. They were analyzed in the Pt4f region. For that purpose, the $Pt4f_{7/2}$:$Pt4f_{5/2}$ doublets were deconvoluted using a least-square curve fitting program based on a mixed 10%/90% Gaussian/Lorentzian function, which accounted for the peak asymmetry, and assuming a 4:3 intensity ratio of the doublet components and a splitting energy of 3.3 eV.

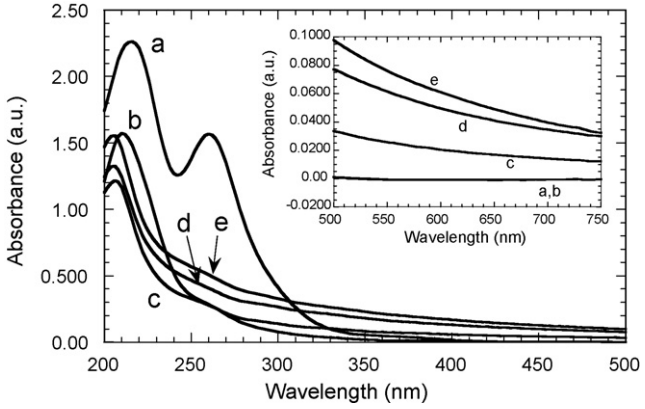

Fig. 1. UV/visible spectra in the short wavelengths region for an 860 μM CPA solution exposed to UV light for 0 min (a), 15 min (b), 60 min (c), 360 min (d), and 900 min (e). Insert shows corresponding spectra in the visible spectral region.

3. Results and discussion

3.1. Photo-induced mechanisms in CPA solution

As-prepared solutions looked transparent slightly yellow. Over UV exposure, their colour progressively turned dark yellow–brown. These colour changes are depicted by UV/visible spectra illustrated in Fig. 1 for an 860 μM CPA solution. For the non-irradiated solution, intense bands initially observed at 215 and 260 nm correspond to metal to ligand charge transfer in a chloro-platinum complex [16]. Two very weak bands are also present at 375 and 460 nm, which cannot be appreciated in spectra of Fig. 1. They are assigned to d → d transitions. Fig. 1 shows that the 260 nm band rapidly decreases in intensity over UV exposure. This band can no longer be detected after 15 min UV exposure. In the same time, the 215 nm band is observed to shift toward 210 nm. Over further UV exposure, this latter band stabilizes at 205 nm and the solution starts to absorb in the whole visible range (see insert of Fig. 1). These latter features are attributed to the formation of platinum metal particles in the solution and are related to MIE scattering effects induced by metal nano-particles [17]. In this study, since the 205 nm band was located at the detection limit of our spectrophotometer, no reliable evolution of this band could be studied over UV exposure. Absorbance evolutions at 260 and 630 nm (this latter wavelength being taken as representative of absorption in the visible spectral range) are plotted in Fig. 2 as a function of UV exposure duration. The 630 nm band remains at zero over an induction period of 15 min, after what it gradually grows with further UV exposure and then saturates in intensity after about 4 h exposure. In the same time, as previously mentioned, absorbance at 260 nm strongly decreases over the first 15 min UV exposure. After what, it slightly increases in intensity with further UV exposure and then saturates after 4 h exposure. It is important to note that these trends did not depend on the presence or not of a TiO_2 sample immersed in the solution during UV exposition. These features suggest, therefore, that UV irradiation induces modifications in the CPA solution, which are not necessarily promoted by photocatalytic mechanisms, as usually

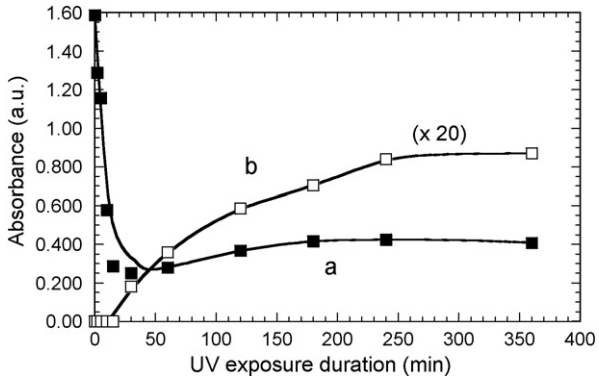

Fig. 2. Absorbance measured at 260 nm (a) and 630 nm (b) for an 860 μM CPA solution exposed to UV light for various durations.

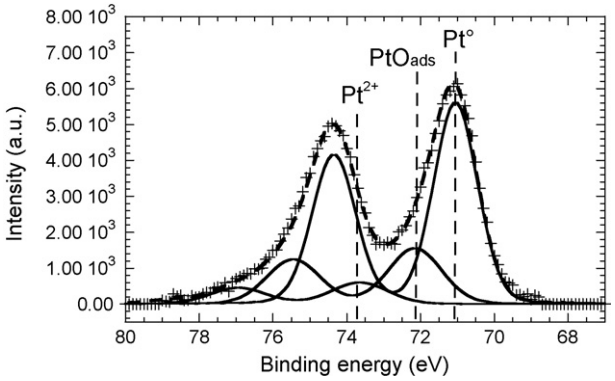

Fig. 3. Typical XPS spectra in the Pt4f region for a TiO_2 film conjointly immersed within a CPA solution and exposed to UV light. "+" symbols indicate the experimental spectrum and lines show the deconvoluted spectra.

proposed to explain processes involved in photo-platinization procedures implemented to functionalize TiO_2 photocatalysts.

Over the past decades, photochemistry of CPA-derived complexes has been the object of numerous studies (see [16,18,19] and articles cited herein). According to these studies, it is known that CPA-derived complexes can undergo a photolytic reduction mechanism through a direct interaction with UV light. This mechanism initially involves a photo-induced homolytic cleavage of the Pt–Cl bond, inducing a first reduction of Pt^{4+} ions and the formation of $Cl^{\bullet}$ radicals. This cleavage can take place in a wide spectral range from 270 to 450 nm. Photo-generated radicals can in turn react with an oxidizable reactant, such as ethanol, yielding new radicals that participate in further reduction of Pt^{4+} ions and induce chain reduction mechanisms. Furthermore, it has been reported that photolytic generation of platinum metal particles only occurs when a large majority of Pt^{4+} ions are transformed into Pt^{2+}ones [19]. Features illustrated in Fig. 2 can be analyzed in the view of aforementioned chain mechanisms. This figure shows that formation of platinum metal particles, as depicted by an absorption onset at 630 nm, is initially not correlated with a decrease of the 260 nm band, attributed to consumption of the CPA precursor. Indeed, while no absorption at 630 nm can initially be appreciated, the CPA consumption rapidly proceeds over the first minutes of UV exposure. This feature probably corresponds to an initial reduction of Pt^{4+} ions into Pt^{2+} ones. Since in the same time the short wavelength band illustrated in Fig. 1 shifts from 215 to 210 nm, it is inferred that this latter location corresponds to Pt^{2+} species. After about 15 min UV exposure, which is attributed to the duration necessary to form a sufficient amount of Pt^{2+}species, appearance of a band at 205 nm and features illustrated in Fig. 2 suggest that the formation of platinum metal particles gradually proceeds. The slight absorbance increase at 260 nm observed in the same time probably ensues from MIE scattering also induced in the UV range by the formation of metal particles. Finally, Fig. 2 suggests that metal particles formation within the solution goes to completion after about 4 h UV exposure.

3.2. Chemical analysis of platinized films

In order to confirm previous interpretations, TiO_2 films immersed in a CPA solution of 860 μM concentration, and exposed to UV light for various durations, have been characterized by EDX and XPS. No XPS spectrum could be exploited for platinization durations shorter than 30 min owing to a too weak signal. For UV exposure duration of 30 min or more, XPS spectra clearly evidence the presence of platinum adsorbed at the TiO_2 surface. A typical XPS spectrum is illustrated in Fig. 3, which depicts three $Pt4f_{7/2}$:$Pt4f_{5/2}$ doublets. In following analyses, we focus on the $Pt4f_{7/2}$ components. For all films studied in the present work, the binding energies of the three $Pt4f_{7/2}$ components were determined to be around 71, 72, and 74 eV. These values fairly agree with previously published works, which assign the three components, from low to high energy, to metallic $Pt^{\bullet}$, Pt with adsorbed oxygen (PtO_{ads}), and oxidized Pt^{2+} [20,21]. As illustrated in Fig. 3, the $Pt^{\bullet}$ component appears to be the most intense one, around 70% of the total Pt4f intensity, showing the strong metallization degree of adsorbed particles. This 70% intensity ratio did not significantly vary in the whole range of UV exposure durations tested with an 860 μM CPA solution (not illustrated here), which indicated the good reduction yield of the corresponding experimental protocol. It should be noted that observation of secondary PtO_{ads} or Pt^{2+} components does not mean that the photo-reduction of Pt^{4+}cations is limited to the +2 valence, but it more probably results from the known tendency of oxygen to rapidly chemisorb on a clean platinum surface during storage under ambient conditions (see further discussion in next section) [20,21]. It is not excluded that non-dissociated residual PtCl species can also partially contribute to the Pt^{2+} component. The photo-platinization kinetics has been studied for TiO_2 films immersed within an 860 μM CPA solution through the variations of the Pt4f integrated intensity normalized to the $Ti2p_{3/2}$ peak (binding energy of 258.7 eV), as deduced from XPS measurements (Fig. 4), and variations of the Pt (Mα)/Ti (Kα) intensity ratio, as deduced from EDX analysis (insert of Fig. 4). On the one hand, the XPS Pt/Ti intensity ratio appears greater when measured with a 30° rather than a 90° take-off angle, which confirms that photo-platinization yields platinum clusters located at the external surface of TiO_2 films. On the

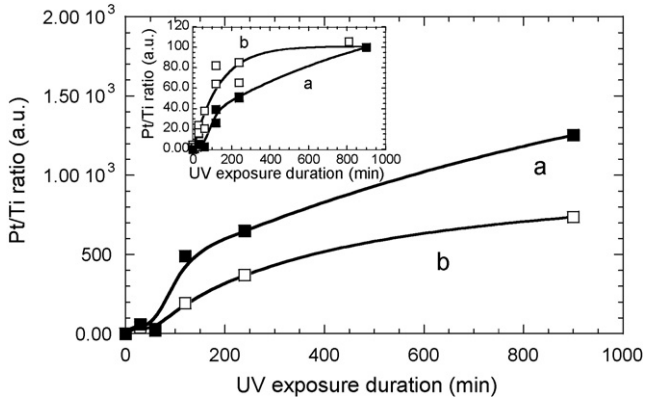

Fig. 4. Pt/Ti intensity ratio deduced from XPS measurements performed at 30° take-off angle (a) and 90° take-off angle (b) for TiO_2 films conjointly immersed within an 860 μM CPA solution and exposed to UV light for various durations. Insert shows similar variations from XPS data (30° and 90° take-off angles are not differentiated) (a), and EDX data (b), after normalization to values measured after 15 h UV exposure.

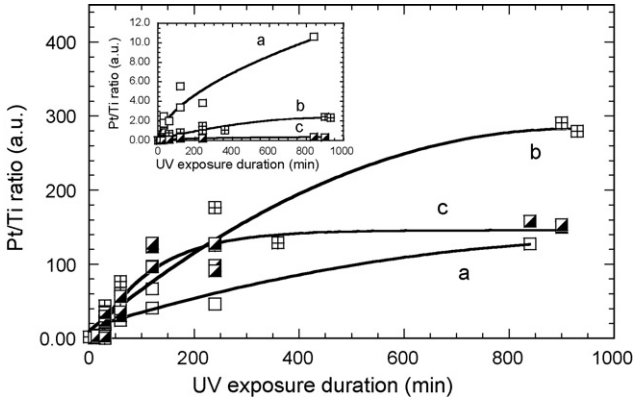

Fig. 5. Pt/Ti intensity ratio deduced from EDX measurements for TiO_2 films conjointly immersed within a CPA solution and exposed to UV light for various durations. CPA concentration in the solution was fixed at 23 μM (a), 230 μM (b), and 860 μM (c). Insert shows similar variations for the Pt/Ti ratio normalized to CPA concentration in the solution.

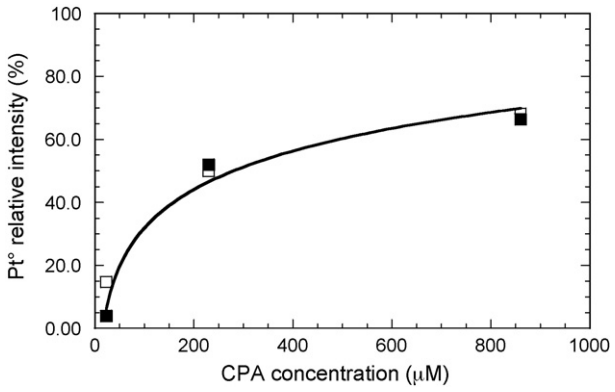

Fig. 6. Pt• peak intensity normalized to the total Pt4f intensity, as deduced from XPS measurements, for TiO_2 films conjointly immersed within CPA solutions of various concentrations and exposed to UV light for 30 min. Measurements have been performed at 30° take-off angle (■) and 90° take-off angle (□).

other hand, XPS and EDX data depict rather similar trends upon UV exposure. The Pt/Ti ratio is initially close to zero, showing that preliminary adsorption of the CPA precursor in the dark occurs in negligible extent. Exposition to UV light induces a bi-regime photoplatinization kinetics. In a first regime, the kinetics is rather fast and, after about 2 h of UV exposure, it significantly slows down. A closer inspection of Fig. 4 shows some differences between XPS and EDX data. The XPS ratio remains very weak over the first hour of UV exposure while the EDX ratio more rapidly increases. Furthermore, slowing down of the platinization kinetics seems to be more marked for the Pt/Ti EDX ratio, which almost saturates after an exposure of 2 h or more. As discussed in next section, these differences can partially be explained with respect to morphology features, taking into account the sample depth probed by XPS and EDX methods.

Similar behaviors were evidenced for solutions of various CPA concentrations exposed to UV light in the presence of a TiO_2 sample. However, the CPA concentration was observed to strongly influence the adsorption kinetics of platinum particles at the TiO_2 surface. EDX data of Fig. 5 indicate that no clear correlation exists between the CPA concentration and the amount of loaded platinum. As previously mentioned, the platinum amount nearly saturates after 2 h UV exposure in the case of the most concentrated solution (860 μM). For the most diluted one (23 μM), the Pt/Ti ratio gradually increases over UV exposure, reaching after 15 h UV exposure a value close to that measured for the most concentrated solution. In the case of a solution with intermediate CPA concentration (230 μM), this ratio also gradually increases, reaching after 15 h UV exposure a value about twice greater than in the case of both other concentrations. These trends can be analyzed in the view of data presented in insert of Fig. 5, which shows evolutions of the EDX Pt/Ti ratio normalized to CPA concentration in the solution. This normalization expresses a platinization yield at the TiO_2 surface. It is observed that this yield strongly increases with decreasing the CPA concentration. As previously explained, ethanol (or any other alcohol) plays an active role in the photolytic reduction of CPA. Reducing the CPA concentration in the solution, i.e. increasing the ethanol to CPA ratio, should logically increase the reduction rate and the yield of platinum particle formation [22]. However, for a strongly diluted solution, the total amount of metal particles is necessarily limited by the weak CPA concentration, which in turn reduces the amount of particles loaded at the TiO_2 surface. In the opposite case, more particles can be formed in a concentrated solution, but the reduction yield should be weaker. An important amount of platinum particles loaded at the TiO_2 surface probably requires, therefore, a compromise in term of CPA concentration, which is expressed by data of Fig. 5. However, data illustrated in Fig. 6 also shows that the Pt• intensity, normalized to the total Pt4f intensity, gradually decreases from 70% to about 10% when decreasing the CPA concentration from 860 to 23 μM, in the case of a CPA solution exposed to UV light for 30 min. Let us recall that, in these experiments, CPA is diluted in a water/ethanol medium of 80/20 molar composition. Thus, decreasing the CPA concentration increases the ethanol to CPA ratio, which should favour a greater reduction yield, but also increases the water to CPA ratio. It is likely that an increased water to CPA ratio counteracts reduction mechanisms, for instance by inducing a more important oxidation at the surface of metal particles. In other words, the photolytic transformation of CPA probably involves complex oxydo-reduction mechanisms that are influenced, among other parameters, by the CPA concentration in the water/ethanol medium. According to these studies, the 860 μM CPA solution appears to be the best compromise in term of reduction efficiency and amount of loaded particles. In the next section, we will thus focus on platinization experiments performed using such a solution.

3.3. Morphological and structural features

Morphological and structural studies of platinum particles provided complementary information yielding new insights into the interpretation of previous chemical analyses and the formation mechanisms of such particles. Fig. 7a–c shows FEG-SEM images of films immersed in a CPA solution and exposed to UV light for 1, 4, and 15 h, respectively. Films exposed for a short duration (1 h or less) were almost exclusively coated with spherical particles, of around 20 nm in diameter, dispersed at the sample surface (Fig. 7a). As illustrated in Fig. 7b, the amount of such particles tends to decrease with further UV exposure. In the same time, small particles of around 2 nm in diameter start to appear, showing a homogeneous distribution at the film surface. After a prolonged UV exposure of 15 h, 20 nm particles can no longer be observed. The TiO_2 film appears to be exclusively coated with 2 nm particles (Fig. 7c). These particles almost coat the totality of the film surface but exhibit a rather disordered distribution. Differences illustrated in Fig. 7b and c probably traduce that, in early platinization stages, 2 nm particles undergo an uniform 2D organisation at the film surface, which progressively evolves toward a less uniform 3D organisation over a too long UV exposure. Morphology changes illustrated in Fig. 7a–c can also explain some differences in EDX and XPS data illustrated in insert of Fig. 4. On the one hand, samples characterized by EDX are probed within a depth of several microns. Thus, the totality of platinum loaded at the TiO_2 surface is accounted for, and data

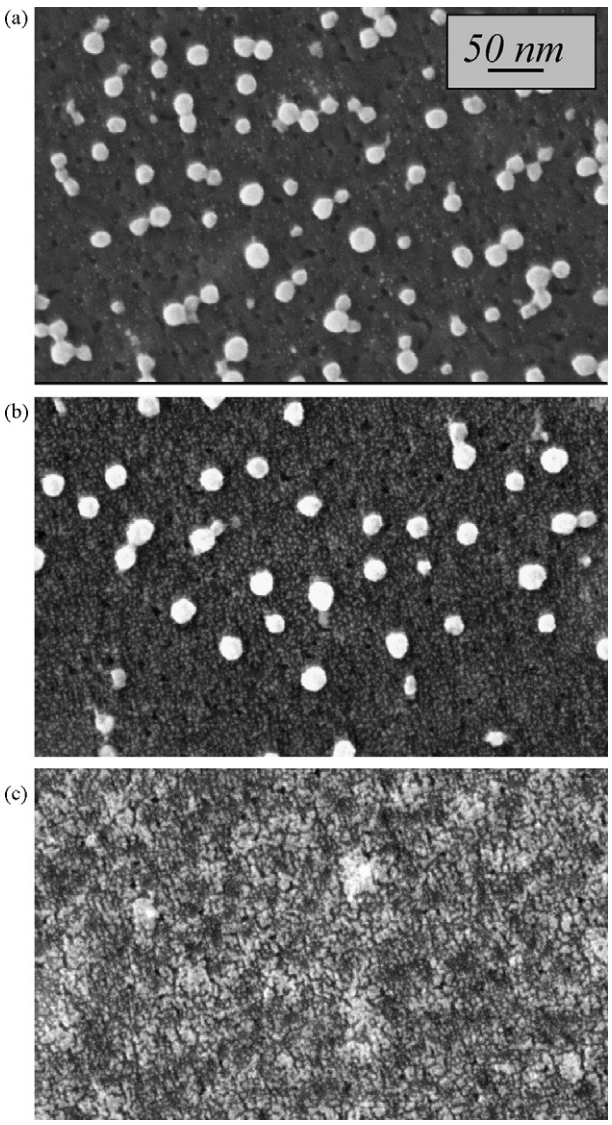

Fig. 7. FEG-SEM images of TiO_2 films conjointly immersed within a CPA solution and exposed to UV light for 1 h (a), 4 h (b), and 15 h (c).

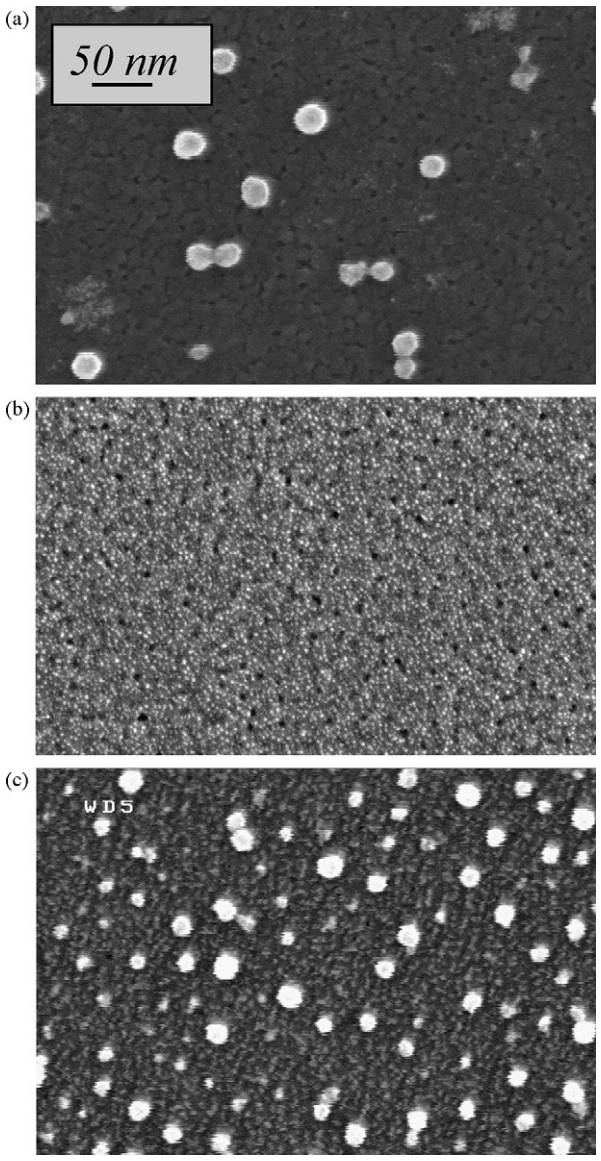

Fig. 8. FEG-SEM images for a TiO_2 film immersed for 45 min within a CPA solution previously exposed to UV light for 45 min (a), for a TiO_2 film immersed for 5 min within a CPA solution previously exposed to UV light for 15 h (b), and for a TiO_2 film which was firstly immersed for 45 min within a CPA solution previously exposed to UV light for 45 min, and was then exposed to UV light for 15 h within a water/ethanol mixture without CPA (c).

illustrated in insert of Fig. 4 indicate a rather fast increase of the platinum amount over the first platinization stages. On the other hand, the depth probed by XPS is limited to a few nanometres. This depth is much smaller than the size of particles loaded over the first platinization stages, which yields an underestimation of the platinum amount. The 20 nm particles are progressively replaced by 2 nm ones while platinization proceeds. The 2 nm size is below the depth probed by XPS. Particles loaded after prolonged platinization are thus more efficiently accounted for by XPS, which yields platinum amount increases illustrated in Fig. 4.

Fig. 8a and b shows FEG-SEM images of films immersed in a CPA solution, which was previously exposed to UV light for 45 min and 15 h, respectively, in the absence of any TiO_2 sample. The former film is coated with particles of around 20 nm diameter, similarly to what is shown in Fig. 7a. This observation seems confirming that the formation of platinum metal particles proceeds through a photolytic (non-photocatalytic) mechanism occurring in the CPA solution, followed by adsorption at the TiO_2 film surface. However, it is important to note that, when the solution was preliminary photolyzed for a short duration, yielding formation of 20 nm particles, post-photolysis adsorption of such particles could be performed in great amount only when the TiO_2 film was exposed to UV light during adsorption. In that case, we cannot exclude that a photocatalytic mechanism also participates to the formation of platinum particles at the TiO_2 surface. Actually, in experiments presented herein, the film is always oriented toward bottom of the glass vessel. It is thus also possible that gravity forces impinge a natural adsorption of rather large platinum particles initially formed in the photolyzed solution. When the film is exposed to UV light, positive and negative charge appear at its surface, due to the photo-induced generation of charge carriers. These surface charges may favour an electrostatic attraction of platinum particles and promote their fixation at the film surface. When exposure of the CPA solution was performed for 15 h, post-photolysis adsorption of the TiO_2 film yielded a very homogeneous distribution of 2 nm particles at the film surface (Fig. 8b). In that case, no significant difference could be observed between morphology features observed after adsorption with or without UV light (not illustrated here). It is possibly due to the very small size of derived platinum particles, which may

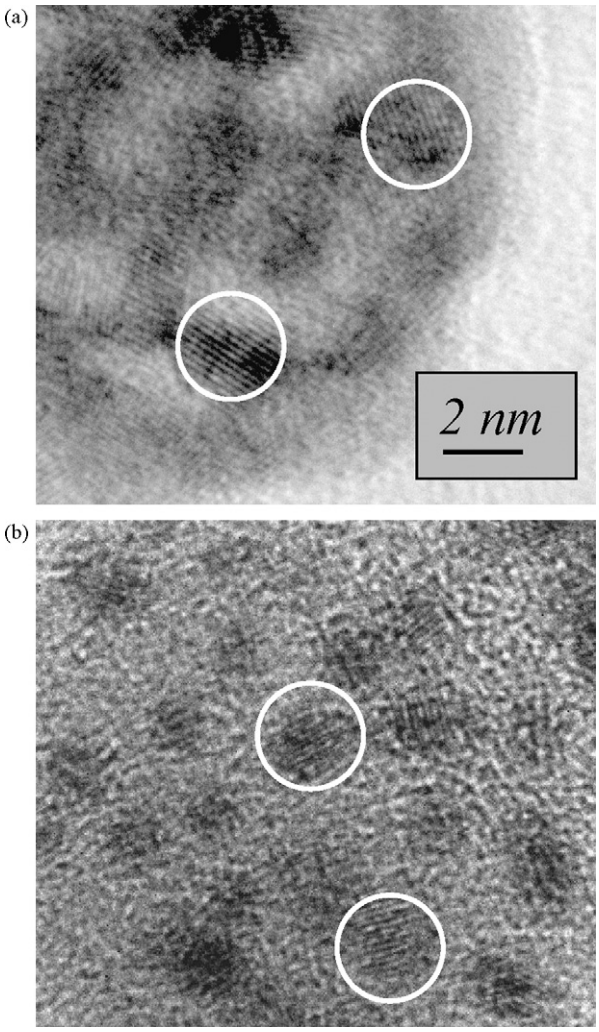

Fig. 9. TEM images of platinum particles derived from a CPA solution exposed to UV light for 45 min (a) and 15 h (b). Circles indicate individual platinum particles.

prevent gravity effects. Moreover, XPS studies showed that particles adsorbed with or without UV light, from solutions previously exposed to UV for 45 min or 15 h, exhibited a similar Pt• component intensity around 70% of the total Pt4f intensity whatever their size (not illustrated here). This value, in agreement with that mentioned in previous section, confirms that photo-induced platinum particles exhibit a strong metallization degree. All these observations definitely prove that formation of platinum particles arises from a photolytic mechanism occurring within the CPA solution. In other words, platinum loading at the TiO_2 surface does not seem involving any photocatalytic reduction but would only rely on a metal particle adsorption mechanism, which can take place either during the solution photolysis, or during a post-photolysis adsorption step.

Previous data show the possibility to form liquid suspensions of metal platinum particles. We took advantage of this feature to disperse such particles on a carbon grid, in order to perform TEM studies. Particles formed after a photolysis of 45 min and 15 h are illustrated in Fig. 9a and b, respectively. After a 15 h photolysis, TEM images confirmed a particle size around 2 nm, and associated electron diffraction pattern confirmed that so-formed particles consisted of crystalline metal platinum (not illustrated here). The crystalline state of platinum is also supported by crystallographic planes observed in Fig. 9b (see circles). After a 45 min photolysis, crystallographic planes can also be observed in Fig. 9a (see circles), and their distribution in various directions indicates that 20 nm particles derived from this solution consist of polycrystalline aggregates. Fig. 9a also shows that single particles constituting these aggregates have a diameter around 2 nm. In other words, these observations indicate that aggregated or not platinum particles always consist of constant size primary particles. It can in turn explain why XPS data yield a constant Pt•/Pt4f intensity ratio of around 70%, whatever the apparent size of platinum particles. Since secondary PtO_{ads} and Pt^{2+} XPS components are assumed to arise from an oxidized particle surface, i.e. the particle would consist of a metallic core surrounded by an oxidized surface shell, the relative amount of oxidized species depends on the surface to volume ratio of the platinum particles, which is in turn determined by the size of primary particles distributed at the film surface or constituting aggregated particles.

Furthermore, it seems that data presented in this article depict a two-step reductive photolytic mechanism occurring in the solution. In a first step, after a sufficient transformation of Pt^{4+} species into Pt^{2+} ones, photolytic reduction might form metal particles of 2 nm diameter, which would rapidly agglomerate into 20 nm aggregates. This fast agglomeration probably arises from the mutual affinity of metal particles diluted in the solution. In a second step, upon prolonged UV exposure, these aggregates would dissociate and regenerate 2 nm particles within the solution. Nano-particles of noble metals exhibit excellent photo-chemical activity, due to a high surface/volume ratio and unusual electronic properties. In the case of silver nano-particles, it has been shown that this photo-chemical activity promotes a fragmentation of metal aggregates when subjected to UV irradiation [23,24]. This mechanism would arise from a photo-induced generation of electrons within silver aggregates, which would destabilize these aggregates and induce their subsequent fragmentation and the formation of smaller metal clusters. It is inferred that data presented in the present article also involve a photo-induced fragmentation of platinum aggregates. Such a fragmentation may occur in the solution exposed to UV light, as previously observed in the case of silver aggregates [23,24], which would explain why samples immersed in a platinum solution previously exposed to UV for 15 h are exclusively coated with 2 nm particles (Fig. 8b). Fragmentation can also take place in particles adsorbed at the TiO_2 surface, which would explain why aggregates adsorbed after the first platinization step (Fig. 7a) are no longer detected after a prolonged UV exposure (Fig. 7c). Of course, photo-chemically induced fragmentation of silver nano-particles is promoted by an absorption band centred around 400 nm [23,24], which is rather close to our UV excitation wavelength (365 nm), while platinum nano-particles essentially absorb at around 200 nm (see Fig. 1), which is much farer from our excitation wavelength. Thus, mechanisms occurring in the fragmentation of silver particles cannot directly be transposed to platinum particles and further studies will be necessary to better assess how fragmentation occurs in our conditions. In order to partially support an eventual UV-induced fragmentation of platinum particles at the TiO_2 film surface, a TiO_2 film has been coated with platinum aggregates formed in a CPA solution photolyzed for 45 min, and then immersed in a water/ethanol solution of 80/20 molar composition, without CPA, and further exposed for 15 h to UV light. Resulting platinum particles are illustrated in the FEG-SEM image of Fig. 8c. It can be seen that 20 nm particles are still present at the TiO_2 surface, in rather important amount, which does not correlate trends illustrated in Fig. 7a and b. However, small particles of 2 nm are also observed at the TiO_2 surface, which were not detected before exposition to UV in the water/ethanol solution (see Fig. 8a). These small particles undergo a surface distribution rather close to that illustrated in Figs. 7b and 8b. These particles cannot be due to adsorption of new platinum cluster, since the latter UV irradiation is achieved in CPA-free water/ethanol solution. This latter observation seems to confirm, therefore, that beside a photo-induced fragmentation

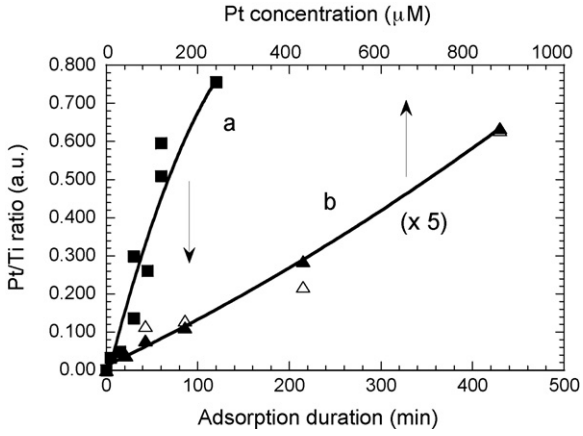

Fig. 10. Pt/Ti ratio deduced from EDX measurements for TiO_2 films immersed for various durations within an 860 μM CPA solution previously exposed to UV light for 45 min (a), and for TiO_2 films immersed for 5 min within CPA solutions of various concentrations, which were previously exposed to UV light for 15 h (b). Immersion of the film was achieved under UV light (■ and △) or not (▲).

occurring within CPA solution, data illustrated in Fig. 7a–c also depict a fragmentation of platinum aggregates that proceeds at the TiO_2 surface exposed to UV light.

This study opens new perspectives in the preparation and applications of platinum nano-particles. In recent years, the preparation of platinum nano-particles in colloidal suspensions has been the object of many studies. Such suspensions are often prepared through chemical [17,22] or photo-chemical routes [16,18]. Experimental protocols generally use a polymeric agent, which participates in the reduction of Pt^{4+} cations and also caps so-formed metal nano-particles thus preventing their fast aggregation and sedimentation in liquid solution. However, presence of this capping agent can also alter the surface properties of metal particles. Fragmentation mechanisms presented herein allow envisaging a new alternative to form stable nano-particles suspensions without the need of any polymeric additive. Furthermore, FEG-SEM images presented above indicate that such suspensions can be homogeneously dispersed at the surface of TiO_2 films through a post-photolysis adsorption mechanism under UV light or not. Fig. 10 also shows that the amount of loaded particles can be flexibly adjusted through a simple control of the adsorption duration and/or platinum concentration in the solution. For instance, in order to quantify a typical amount of 2 nm particles that can selectively be loaded at the film surface through a post-photolysis adsorption, XPS studies have been performed on a sample immersed under UV light for 5 min within an 860 μM CPA solution which was previously photolyzed for 15 h. XPS data, corrected from the sensitivity factor of titanium and platinum, yield an apparent Pt/Ti surface atomic percentage of 160% (30° take-off angle) or 100% (90° take-off angle). Since a post-photolysis adsorption protocol allows to selectively disperse 2 or 20 nm at the TiO_2 films surface, it will be also interesting in further studies to investigate how the dispersion of aggregated or individual particles influences the photocatalytic activity of TiO_2 films, in relation to the amount of loaded particles. Finally, since no photocatalytic mechanism is a priori involved in the surface platinum loading, it is inferred that platinum nano-particles can be dispersed at the surface of any support. Accordingly, we could homogeneously disperse 2 nm particles at the surface of an indium tin oxide film (ITO, not illustrated here), which can present interests for various applications such as new electrode materials [25]. However, it is worthwhile mentioning that, in similar adsorption conditions, platinum dispersion at ITO surface yielded a much smaller amount of particles than adsorption at TiO_2 surface. This observation suggests that the adsorption conditions may be influenced by the affinity of platinum particles for the support, which can in turn depend on surface properties of this support, such as morphology or surface chemistry. Accordingly, we could also adsorb platinum particles at SiO_2 surfaces (sol–gel-derived film or native oxide present at the surface of a Si wafer) but, contrary to the cases of TiO_2 or ITO supports, these particles appeared to be much less homogeneously dispersed.

4. Conclusion

Sol–gel TiO_2 photocatalytic thin films have been loaded with platinum nano-particles via their immersion within a CPA liquid solution exposed to UV light. This study shows that formation and dispersion of metal platinum particles proceeds through a photolytic reduction mechanism, occurring in the platinum precursor solution, rather than a photocatalytic reduction at the TiO_2 surface. This mechanism offers an easy way to prepare platinum nano-particles in liquid suspension that can subsequently be dispersed on various kinds of supports. Photolytic reduction mechanisms have been studied using various characterization methods. These studies show the possibility to selectively disperse platinum particles of 2 or 20 nm diameter in controlled amount. Platinum adsorption protocols derived from such photolyzed solutions allow envisaging not only enhanced photocatalytic activity of TiO_2 thin films, as shown in our previous work [13], but also opens the way to new applicative studies.

References

[1] C. He, Y. Xiong, X. Zhu, X. Li, Appl. Catal. A: Gen. 275 (2004) 55.
[2] M. Zhang, Z. Jin, J. Zhang, Z. Zhang, H. Dang, J. Mol. Catal. A: Chem. 225 (2005) 59.
[3] M. Zhang, Z. Jin, Z. Zhang, H. Dang, Appl. Surf. Sci. 250 (2005) 29.
[4] S.C. Kim, M.C. Heo, S.H. Hahn, C.W. Lee, J.H. Joo, J.S. Kim, I.K. Yoo, E.J. Kim, Mater. Lett. 59 (2005) 2059.
[5] D. Lahiri, V. Subramanian, B.A. Bunker, P.V. Kamat, J. Chem. Phys. 124 (2006) 124.
[6] M. Sadeghi, W. Liu, T.-G. Zhang, P. Stavropoulos, B. Levy, J. Phys. Chem. 100 (1996) 19466.
[7] K.T. Ranjit, B. Viswanathan, J. Photochem. Photobiol. A: Chem. 108 (1997) 73.
[8] J.C. Kennedy III, A.K. Datye, J. Catal. 179 (1998) 375.
[9] A. Yamakata, T. Ishibashi, H. Onishi, J. Phys. Chem. B 105 (2001) 7258.
[10] U. Siemon, D. Bahnemann, J.J. Testa, D. Rodriguez, M.I. Litter, N. Bruno, J. Photochem. Photobiol. A: Chem. 148 (2002) 247.
[11] J.M. Herrmann, J. Disdier, P. Pichat, A. Fernandez, A. Gonzalez-Elipe, G. Munuera, C. Leclercq, J. Catal. 132 (1991) 490.
[12] O. Carp, C.L. Huisman, A. Reller, Prog. Solid State Chem. 32 (2004) 33.
[13] C. Millon, D. Riassetto, G. Berthome, F. Roussel, M. Langlet, J. Photochem. Photobiol. A: Chem. 189 (2007) 334.
[14] M. Fallet, S. Permpoon, J.L. Deschanvres, M. Langlet, J. Mater. Sci. 41 (10) (2006) 291.
[15] M. Langlet, S. Permpoon, D. Riassetto, G. Berthomé, E. Pernot, J.C. Joud, J. Photochem. Photobiol. A: Chem. 181 (2–3) (2006) 203.
[16] M. Harada, K. Okamoto, M. Terazima, Langmuir 22 (2006) 9142.
[17] C.W. Chen, D. Tano, M. Akashi, Colloid Polym. Sci. 277 (1999) 488.
[18] W. Macyk, H. Kisch, Chem. Eur. J. 7 (2001) 1862.
[19] R.E. Cameron, A.B. Bocarsly, Inorg. Chem. 25 (1986) 2910.
[20] B. Ohtani, K. Iwai, S.-I. Nishimoto, S. Sato, J. Phys. Chem. B 101 (1997) 3349.
[21] K.S. Kim, N. Winograd, R.E. Davis, J. Am. Chem. Soc. 92 (23) (1971) 6296.
[22] T. Teranishi, M. Hosoe, T. Tanaka, M. Miyake, J. Phys. Chem. B 103 (1999) 3818.
[23] P.V. Kamat, M. Flumiani, G.V. Hartland, J. Phys. Chem. B 102 (1998) 3123.
[24] S.K. Ghosh, S. Kundu, M. Mandal, S. Nath, T. Pal, J. Nanopartic. Res. 5 (2003) 577.
[25] G. Chang, M. Oyama, K. Hirao, J. Phys. Chem. 110 (2006) 1860.